Symmetry breaking yields chimeras in two small populations of Kuramoto-type oscillators

Oleksandr Burylko[1,2], Erik A. Martens[3,4], and Christian Bick[5,6]

[1]Institute of Mathematics, NAS of Ukraine, Kyiv
[2]Potsdam Institute for Climate Impact Research, Germany
[3]Lund University, Sweden
[4]Technical University of Dresden, Germany
[5]Vrije Universiteit Amsterdam, the Netherlands
[6]University of Exeter, United Kingdom

University of Exeter, 23 June, 2022

Modular network: M populations of N oscillators

$L = MN$ phase oscillators

M identical populations
N oscillators in each population

$$\dot{\theta}_{\sigma,k} = \omega + \frac{K_s}{MN}\sum_{j=1}^{N}\sin(\theta_{\sigma,j} - \theta_{\sigma,k} - \alpha_s) + \frac{K_n}{MN}\sum_{\tau\neq\sigma}\sum_{j=1}^{N}\sin(\theta_{\tau,j} - \theta_{\sigma,k} - \alpha_n). \quad (1)$$

$\theta_{\sigma,k} \in \mathbb{T}$ – phase of the oscillator $k \in \{1,\dots,N\}$ in population $\sigma \in \{1,\dots,M\}$

ω – natural frequency

K_s – coupling strength within population
K_n – coupling strength between populations
$\alpha_s \in \mathbb{T}$ – phase shift within population
$\alpha_n \in \mathbb{T}$ – phase shift between populations

By rescaling time we can set $K_s + K_n = 1$ and introduce:

$$A := K_s - K_n$$

$K_s = K_n$ $(A = 0)$, $\alpha_s = \alpha_n$ – Kuramoto-Sakaguchi model

Two-modular network of four phase oscillators

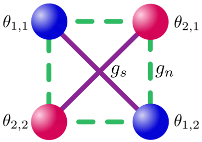

$$
\begin{aligned}
\frac{d\theta_{1,1}}{dt} &= \omega + g_s(\theta_{1,1} - \theta_{1,2})/4 + [g_n(\theta_{1,1} - \theta_{2,1}) + g_n(\theta_{1,1} - \theta_{2,2})]/4, \\
\frac{d\theta_{1,2}}{dt} &= \omega + g_s(\theta_{1,2} - \theta_{1,1})/4 + [g_n(\theta_{1,2} - \theta_{2,1}) + g_n(\theta_{1,2} - \theta_{2,2})/4, \\
\frac{d\theta_{2,1}}{dt} &= \omega + g_s(\theta_{2,1} - \theta_{2,2})/4 + [g_n(\theta_{2,1} - \theta_{1,1}) + g_n(\theta_{2,1} - \theta_{1,2})]/4, \\
\frac{d\theta_{2,2}}{dt} &= \omega + g_s(\theta_{2,2} - \theta_{2,1})/4 + [g_n(\theta_{2,2} - \theta_{1,1}) + g_n(\theta_{2,2} - \theta_{1,2})]/4,
\end{aligned} \tag{2}
$$

$$
g_s(\phi) = -K_s \sin(\phi - \alpha_s), \quad g_n(\phi) = -K_n \sin(\phi - \alpha_n), \tag{3}
$$

K_s, K_n, α_s, α_n – parameters (new parameter $A := K_s - K_n$)

Phase differences:

$$
\psi_1 = \theta_{1,1} - \theta_{1,2}, \quad \psi_2 = \theta_{1,2} - \theta_{2,1}, \quad \psi_3 = \theta_{2,1} - \theta_{2,2} \tag{4}
$$

Invariant manifolds in 3D torus

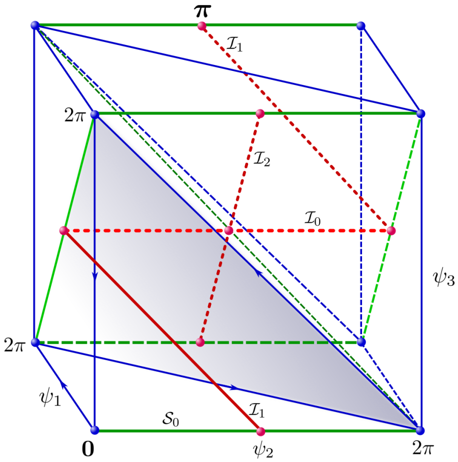

Invariant manifolds in phase space of variables $(\psi_1, \psi_2, \psi_3) \in \mathbb{T}^3$ for system (2), (3) of four coupled oscillators. The system has six *canonical invariant manifolds* in Kuramoto-Sakaguchi case: $K_s = K_n = K$ $(A = 0)$ and $\alpha_s = \alpha_n = \alpha$. Four of the six invariant planes and blue invariant lines disappear with permutational symmetry breaking.

Symmetries

Dihedral symmetry $\mathbf{D}_4$ for system in phase differences is given by actions:
rotation

$$\gamma_{\mathrm{r}}: \ (\psi_1, \psi_2, \psi_3) \mapsto (-\psi_3, -\psi_1 - \psi_2, \psi_1),$$

and mirror (reflection)

$$\gamma_{\mathrm{m}}: \ (\psi_1, \psi_2, \psi_3) \mapsto (\psi_1, \psi_2 + \psi_3, -\psi_3).$$

Parameter symmetries:

$$\gamma^{(\alpha_n)}: \ (\psi_2; \alpha_n) \mapsto (\psi_2 + \pi; \alpha_n + \pi),$$

$$\gamma^{(A,t)}: \ (\psi_2; A, t) \mapsto \begin{cases} (\psi_2 + \pi; 1/A, t), & A > 0 \\ (\psi_2 + \pi; 1/A, -t), & A < 0 \end{cases}$$

Critical cases:

1. $K_s = K_n = K$ $(A = 0)$, $\alpha_a = \alpha_n = \alpha$ – Kuramoto-Sakaguchi model with permutational symmetry $\mathbf{S}_4$
2. $K_n = 0$ $(A = 1)$ – two uncoupled populations
3. $K_s = 0$ $(A = -1)$ – ring network (no couplings inside populations)
4. $\alpha_s = \alpha_n = \pm\pi/2$ – conservative dynamics

Phase configurations of different collective regimes

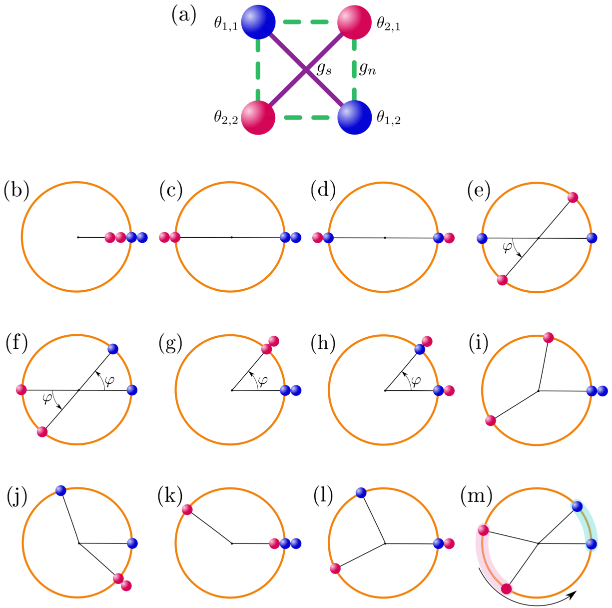

Invariant manifolds in 3D torus

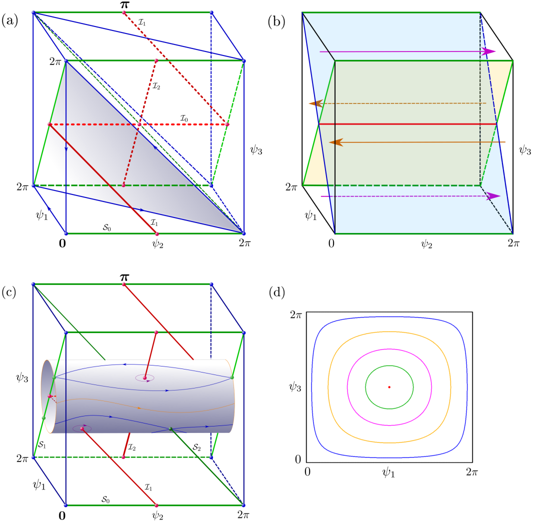

Schematic representation of invariant manifolds in variables $(\psi_1, \psi_2, \psi_3) \in \mathbb{T}^3$ for system (2), (3). **(a)** Kuramoto-Sakaguchi case; **(b)** Two uncoupled groups ($K_n = 0$); **(c)** Invariant surface in conservative case; **(d)** Level lines of the first integral.

Schematic phase portraits on the invariant cylinder ($\alpha_s = \alpha_n = \pm\pi/2$)

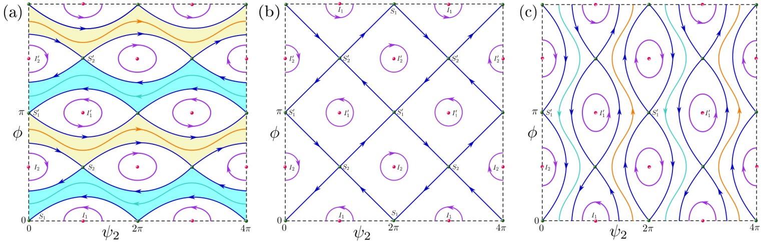

Dynamics on cylinder $L(C)$ is presented in variables (ψ_2, ϕ), where $\phi \in \mathbb{T}^1$ is an angle that parametrizes the curve

$$H^{(\cdot,\pi/2)}(\psi_1, \psi_3) = \sin\frac{\psi_1}{2}\sin\frac{\psi_3}{2} = C,\ \ C \in [0,1].$$

Critical cylinder size

$$C^* = \begin{cases} \dfrac{2A}{A+1}, & A \in [0,1], \\[2ex] \dfrac{2}{A+1}, & A \geq 1, \end{cases}$$

Weak chimeras for $C \in (0, C^*)$;
Heteroclinic web for $C = C^*$;
Frequency locked solutions for $C \in (C^*, 1)$.

Serpentine chimera in two-modular system (heteroclinic surface)

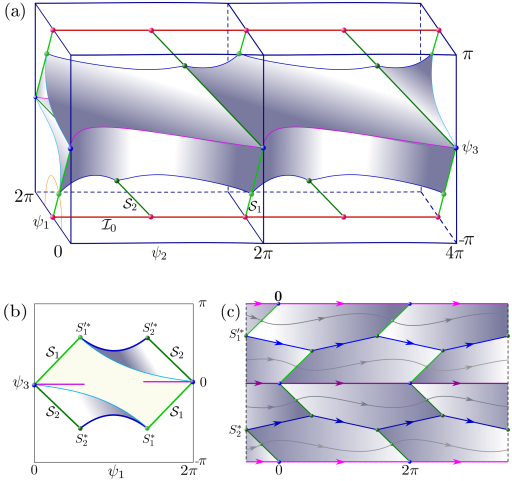

Schematic representation of "serpentine chimera" in variables $(\psi_1, \psi_2, \psi_3) \in \mathbb{T}^3$.
(a) The structure of the boundary surface (grey) for neutral periodic *chimera states* (phase unlocked along ψ_2 periodic solutions in $\mathbb{T}^3$). **(b)** Projection into (ψ_1, ψ_3) plane. **(c)** "Skin of the chimera-snake" – dynamics on the surface of boundary chimera surface (the map from the surface to a plane).

$$A := K_s - K_n : \; K_s + K_n = 1$$

Statement 1. In the case $\alpha_s = \alpha_n = \pm\pi/2$ system (2) is divergence-free for any A.

Statement 2. In the case $\alpha_s = \alpha_n = 0$ system (2) is a gradient system for any A.

The first integrals:

$$H^{(\cdot,\frac{\pi}{2})} = \sin\frac{\psi_1}{2}\sin\frac{\psi_3}{2}, \qquad \alpha_s = \alpha_n = \pm\pi/2,\ \forall A$$

$$H^{(1,\cdot)} = \cot\frac{\psi_1}{2}\tan\frac{\psi_3}{2}, \qquad A = 1,\ \forall \alpha_s, \alpha_n$$

$$H^{(1,0)} = \psi_1 + 2\psi_2 + \psi_3, \qquad A = -1, \alpha_s = \alpha_n = \pm\pi/2 \text{ or } A = 1, \alpha_s = \alpha_n = 0$$

$$H^{(-1,0)} = \cot\frac{\psi_1 + \psi_3}{4}\tan\frac{\psi_1 - \psi_3}{4}, \qquad A = -1, \alpha_s = \alpha_n = 0 \text{ or } \alpha_s = \pi/2, \alpha_n = 0, \forall A$$

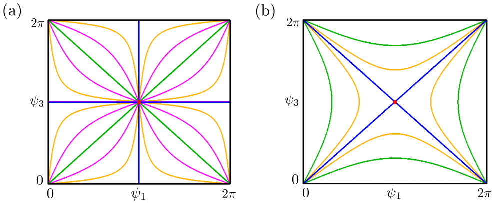

Conservative-dissipative dynamics (for $\alpha_s = \pi/2$, $\alpha_n = 0$, $\forall A = K_s - K_n$)

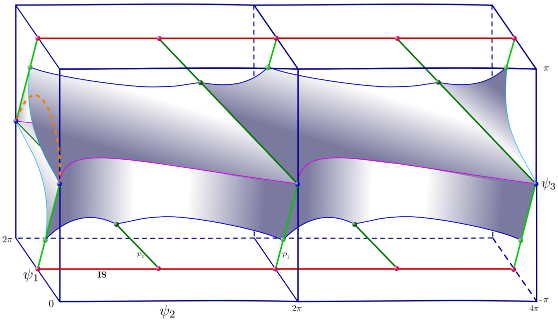

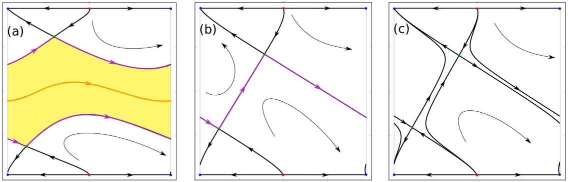

Schematic phase portraits on the cylindric surfaces $H^{(-1,0)} = C$ are shown for variables $(\psi_2, \phi) \in \mathbb{T}^2$. (a)-(c) Bifurcation transition leads to the disappearance of the conservative region (shaded in yellow) filled with periodic (chimera) trajectories.

Flat chimeras (synchronization inside one cluster), $\psi_1 = 0$ or $\psi_3 = 0$

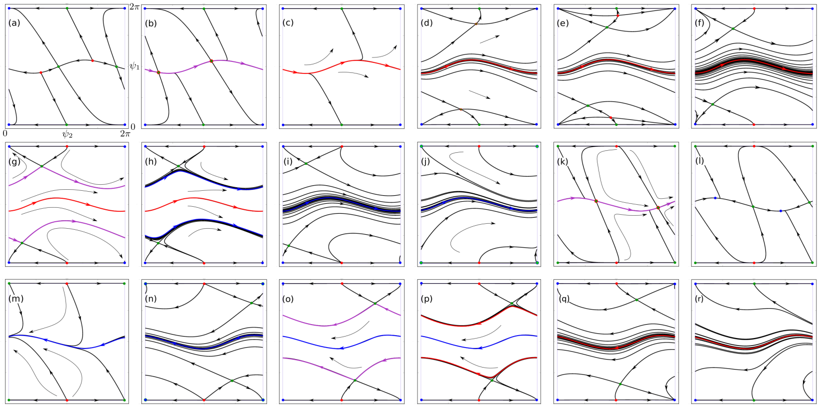

Phase portraits on the invariant surface $\psi_3 = 0$ for $(\psi_2, \psi_1) \in [0, 2\pi]^2$ show the bifurcation behavior for increasing parameter $\alpha_s \in [0, 2\pi]$ keeping $A = K_s - K_n = 0.7$, $\alpha_n = 0.44$ fixed.

Notations: sink and stable limit cycle (blue), source and unstable limit cycle (red), saddle (green), saddle-node (two-color), homo/heteroclinic cycle (magenta).

Chaotic chimeras

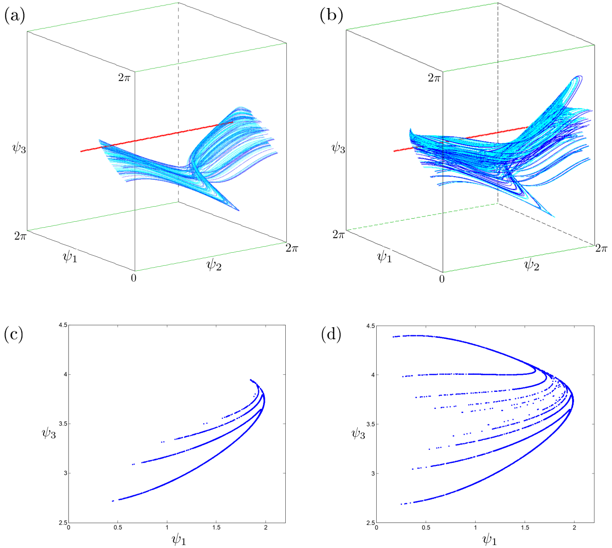

(a), **(b)** Chaotic trajectory of the system (2), (3) for $\psi_1, \psi_2, \psi_3 \in [0, 2\pi]^3$, $A = 0.7$, $\alpha_n = 0.44$, $\alpha_s = 1.6415$ and $\alpha_s = 1.64166$. **(c)**, **(d)** Poincaré sections $\psi_2 = \pi$ for (a) and (b).

Chaotic chimeras

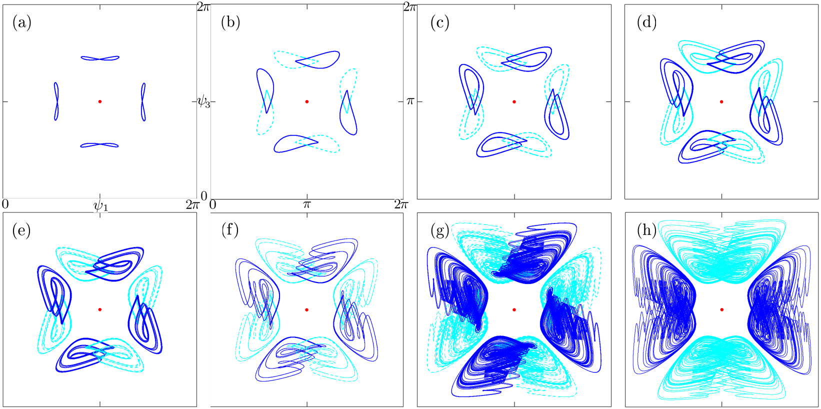

Projections of *periodic and chaotic chimeras* into the plane $(\psi_1, \psi_3) \in [0, 2\pi]^2$ for fixed $A = 0.7$, $\alpha_n = 0.44$ and increasing $\alpha_s \in [1.58, 1.64]$. (a) self-symmetric eight-shape stable limit cycles; (b) pairs of stable limit cycles (blue and cyan) that emerge from eight-shaped ones; (c)-(f) limit cycles that emerge after a chain of the period-doubling bifurcations; (g) eight symmetric chaotic attractors; (h) four symmetric chaotic attractors that appear after a symmetry increasing bifurcations of pairs of smaller chaotic chimers.

Chaotic chimeras

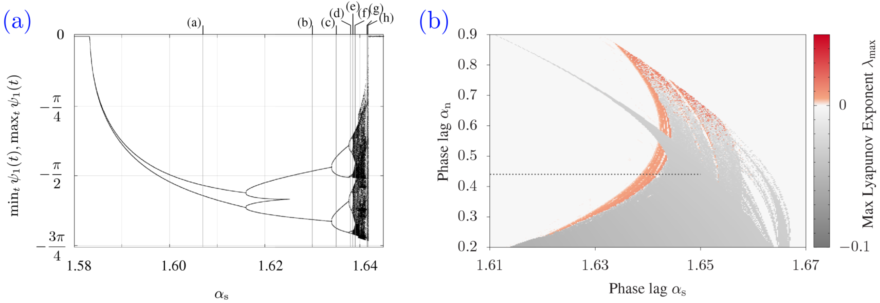

The road to chaotic weak chimeras. **(a)** shows a bifurcation diagram obtained via quasi-continuation for fixed $A = 0.7$ and $\alpha_s = 0.44$. Vertical lines delineate α_s-values for the trajectories shown on the previous slide.
(b) shows the maximal Lyapunov exponent for varying (α_s, α_n) calculated by numerically integrating from a fixed initial condition for $T = 10000$ time units. The dashed line indicates parameter values shown in (a)

Minichimerapedia for networks of two populations of two phase oscillators

1. Limit cycle solutions on the invariant planes $\psi_1 = 0$ or $\psi_3 = 0$, referred to as flat chimeras. The situation corresponds to phase synchronization of one of the populations with local order parameter $|Z_1| = 1$ (or $|Z_2| = 1$) and $|Z_2(t)| \in (0, 1)$ (or $|Z_1(t)| \in (0, 1)$).
2. A one-parameter family of periodic orbits on the invariant plane for $\alpha_s = \pm\frac{\pi}{2}$ and $\alpha_n = 0$, $\alpha_n = \pm\frac{\pi}{2}$, $\alpha_n = \pi$.
3. A two-parameter family of neutrally stable periodic orbits (3D conservative region).
4. The four 8-shaped symmetric limit cycles.
5. The eight limit cycles without symmetry.
6. The eight nonsymmetric chaotic attractors.
7. The four symmetric chaotic attractors
8. The surface of the heteroclinic orbits (serpantine chimera) that bound the conservative family of the periodic orbits

Proposition. System (1) is divergence-free in the case of *even* coupling function $g_s(\phi) = g_n(\phi) = g(\phi)$.

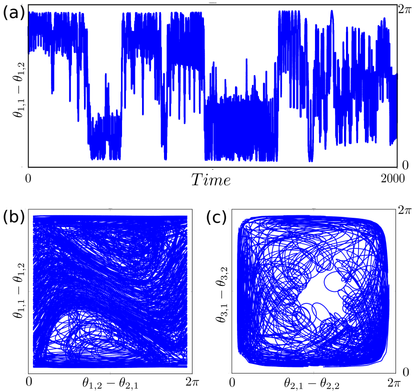

Example of a neutral chaotic weak chimera in the six oscillator system for $M = 3$, $N = 2$ in the conservative case $\alpha_s = \alpha_n = \frac{\pi}{2}$, $A = \frac{1}{2}$. (a) Time series of phase difference between two oscillators of the first group. (b) and (c): Projections of trajectories from $\mathbb{T}^5$ into phase planes of the phase differences.

Summary

- Modular system (1) has dihedral symmetry $\mathbf{D}_{MN}$ for any M and N instead of full permutational symmetry $\mathbf{S}_{MN}$ for global coupling.
- Symmetry breaking ($K_s \neq K_n$, $\alpha_s \neq \alpha_n \implies \mathbf{S}_{MN} \to \mathbf{D}_{MN}$) destroys clusters (invariant manifolds) from different populations and does not destroy clusters from the same population
- Bifurcations transition from global Kuramoto-Sakaguchi system to modular oscillator network leads to emergence of weak chimera states
- System of four oscillators has many types of the weak chimera solutions: periodic, chaotic, heteroclinic, two parameter family of neutral periodic solutions, family (surface) of homo/heteroclinic orbits (serpentine chimera)
- Modular system (1) has a continuous set of neutral chimera solutions in the case $\alpha_s = \alpha_n = \pm\pi/2$. These solutions can be periodic, quasi-periodic or chaotic (similar to ABC flows)
- System can have conservative-dissipative dynamics for even $g_s(\phi)$ and odd $g_n(\phi)$